A Dynamic Multi-Link MIMO Measurement System for 5.3 GHz

P. Almers[†], *K. Haneda*[*], *J. Koivunen*[*], *V.-M. Kolmonen*[*], *A. F. Molisch*[†§],
A. Richter[‡], *J. Salmi*[‡], *F. Tufvesson*[†], *P. Vainikainen*[*]

[*]TKK Helsinki University of Technology, SMARAD Radio Laboratory, Finland
[†]Lund University, Dept. of Electrical and Information Technology, Sweden
[‡]TKK Helsinki University of Technology, SMARAD Signal Processing Laboratory, Finland
[§]Mitsubishi Electric Research Laboratories (MERL), Cambridge, MA, USA

Email: peter.almers@eit.lth.se

Abstract

Multi-link MIMO systems, including multi-user MIMO and MIMO with base station cooperation, are essential parts of high-throughput wireless LANs and fourth-generation cellular systems. In order to fully understand such systems, the dynamic channel characteristics of multi-link MIMO channels have to be measured. In this paper we present a measurement setup that enables such measurements and does not suffer from the deficiencies of previous, "virtual multi-user" setups. We also present sample results from a measurement campaign with this setup at 5.3 GHz in an indoor office environment.

1 Introduction

With the constantly growing requirement for higher data rates, multiple-input multiple-output (MIMO) technology has drawn huge attention from the wireless community during the last ten years [1, 2, 3]. Already today some WLAN products (e.g., Draft IEEE 802.11n) utilizing the MIMO technology are available. Until recently, it has mostly been *single-link* MIMO systems that have been studied and shown to provide tremendous benefits. However, as the user density in different wireless networks such as WLAN and WiMAX is increasing, the need to understand the effects of multi-user interference in multi-link MIMO scenarios is growing, and a number of papers has been published about (i) MIMO with multiple users in a single cell (see, e.g., [4], [5], [6]), (ii) capacity of interference-limited MIMO systems without coordination [7], and (iii) interference-limited systems with base station cooperation [8]. However, those papers deal with idealized, and in general uncorrelated, channels.

In order to fully understand the implications of multi-link MIMO, measurements and models for the multi-link MIMO propagation channels are required. As of now, there exist only some *static* multi-link MIMO measurements, where several, subsequently taken, single-link MIMO measurements are used to form a static multi-link scenario (see, e.g., [9]). However, such an approach is not valid if parts of the channel changes (due to, e.g., movements of people, cars etc.) between measurements at different locations. In the current paper we describe a measurement setup capable of measuring the *dynamic* multi-link MIMO channel. We will also show the capabilities of our measurement setup with some sample results. To the best of our knowledge, this is the first dynamic multi-link MIMO measurement campaign published (some results from this campaign were reported in [10]).

2 Dynamic Multi-link Measurement System

In this section the joint sounder measurement setup is presented (see Fig. 1). It consists of two channel sounders from two different institutions (TKK and Lund University) that have been appropriately modified to work together.

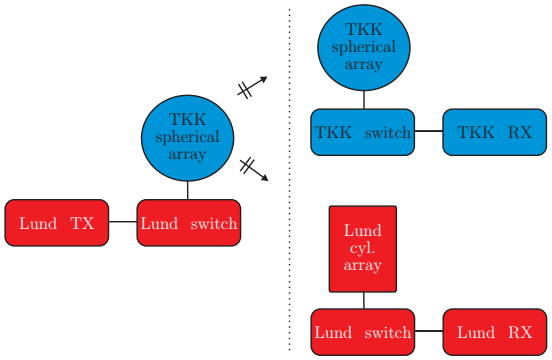

Fig. 1. Block diagram of the dual-sounder measurements setup.

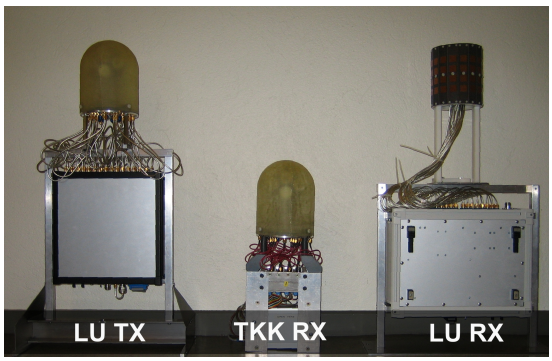

Fig. 2. Picture of the antenna structures and switches.

2.1 The LU and TKK Sounders Description

The Lund University (LU) sounder is a commercial wideband MIMO channel sounder, RUSK LUND, from MEDAV GmbH [11, 12]. The transmitter (TX) of the LU sounder has an arbitrary waveform generator unit for generating periodic multi-frequency signals with a signal length of 1.6 μs (can be extended in multiples of 1.6 μs up to 25.6 μs). The LU receiver (RX) and LU TX are synchronized, i.e., the local oscillators are phase locked either to one common 10 MHz reference or to local rubidium clocks that are frequency synchronized/tuned [13]. Further, the RX is synchronized to the transmit signal and the fast RF-switches at the TX and RX are also synchronized. A guard period is used when the element switching take place at the RX, hence with a signal length of 1.6 μs one of the channels between the antenna pairs is measured each 3.2 μs. However, the MIMO channel transfer function was sampled each 39.32 ms, due to data buffering limitations. A back-to-back calibration is made before the measurement, in order to remove the influence of the measurement system on the measurements.

For the TKK sounder, only the RX unit is used, which basically is a down converter and sampling unit [14]. All signal processing, including correlation of the received signal with the transmitted signal, is performed in the post processing process. Hence, the post-processing can be easily adjusted for various types of sounding signals. The TKK RX is not synchronized with the LU TX switch nor to the transmit signal. The TKK RX also measures the LU TX signal in a back-to-back measurement in order to store the transmit signal waveform used in the post-processing.

It is possible to adjust the bandwidth (here 120 MHz) and center frequency of the LU TX to match the parameters of of the TKK RX, so that the transmitted signal can be measured with the sampling rate of the TKK RX without aliasing.

2.2 Synchronization

There are different levels of synchronization. Synchronization of TX signal, synchronization of antenna switching and synchronization of MIMO snapshots is not possible between the LU TX and the TKK RX, which introduces a couple of issues that had to be solved.

1) The transmit signals of the two TXs can not be synchronized, orthogonallity between transmitted signals (e.g., TDD) is not possible for a fast system. The measurement configuration is then limited to one TX and two RXs, as shown in Fig. 1, which is capable of measuring the dynamic *point-to-multi-point* and also *multi-point-to-point* MIMO channels (assuming channel reciprocity).
2) The LU TX signal is not synchronized to the TKK RX, and therefore there is no common time reference between the LU and TKK channels, see Fig. 3. The difference in time reference is not known, but will stay constant during a measurement and also between the measurements and is adjusted for in the post-processing stage.
3) The LU TX switch and the TKK RX switch are not synchronized, resulting in that the channels are mixed up. This was solved by using a *matched load* at one of the LU TX output channels and at one of the TKK RX input channels, which makes it possible to synchronize the switching patterns in the post-processing using these *dummy channels*.
4) The start of a measurement is not synchronized between the LU TX and the TKK RX, hence the mapping of the MIMO snapshots of the LU TX with the MIMO snapshots of the TKK RX was solved by using a switch at the LU TX. Hence, in all of the measurements the TX power was switched on shortly after the sampling was started at both the RXs. Using the snapshots where the power is switched on as a reference, the MIMO snapshots of the TKK RX and LU TX could be synchronized in the post-processing step.

2.3 Antenna Arrays

The antennas used for the measurements are shown in Fig. 2. The cylindrical antenna structure used for the LU RX consists of 4 rings of 8 dual polarized antenna elements, and so the antenna has 64 dual polarized (horizontal and vertical) antenna elements in total. From these, 16 dual polarized elements were used; 8 elements from each of the two middle rows were selected in an alternating fashion.

The semi-spherical antenna structure for the TKK RX has 21 dual polarized (horizontal and vertical) elements, of which 15 dual polarized elements are connected to the switch. In addition to these 30 channels a discone antenna (connected to the AGC controller of the TKK RX) and a dummy channel (for synchronization discussed previously) were used both at the LU TX and at the TKK RX.

The semi-spherical antenna structure used for the LU TX is identical to the one used in the TKK RX, except the polarization of the dual polarized elements is different (45° slanted).

All unused antenna elements were terminated using matched loads.

2.4 Post-Processing

The measured data have to be post-processed to obtain MIMO- channel transfer functions (MIMO-CTF) for both links. Since the switching cycle of the LU-RX was synchronized with the LU-TX switching cycle the MIMO-CTF for this link is directly estimated from the measured data. For the other link first the offset between the TX switching cycle and the RX switching cycle has to be estimated. The procedure used is described in the following.

1) Channel Synchronization: Each of the M_R ports at the TKK RX is measured between the TX switching times. For the inactive TX antenna, this yields M_R inactive channels at the RX. The inactive TX antenna is detected using a moving average of the received power, yielding a sufficiently accurate estimate of the offset between the TX and the RX switching frame.

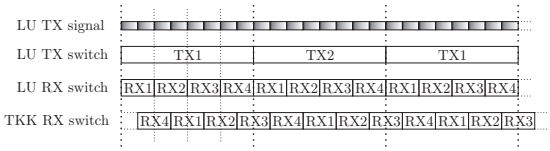

Fig. 3. Synchronization between LU and TKK sounders shown for 2 TX and 4 RX elements.

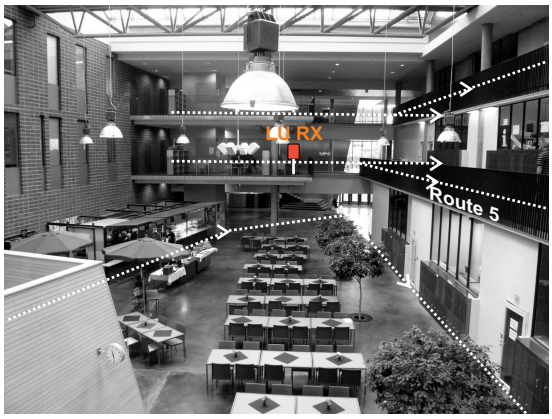

Fig. 4. The picture is taken from one of the TKK RX's positions showing one of the LU RX positions and parts of the TX routes.

2) Signal Synchronization: The TX switching takes place at an arbitrary (but constant) position inside one of the measured TKK RX channels. Because two signal lengths ($2 \cdot 1.6$ μs) are measured for each channel, it is (in most cases) possible to minimize the TX switching effect by extracting the signal at a proper position inside the two sequences. The optimal sequence position is determined by selecting the interval of 1.6 μs within the 3.2 μs, which minimizes the MSE to the adjacent samples. If only the RX-antenna element has been switched, this approach will yield the channel measurement with the smallest distortion due to the settling time of the receiver. However, if the TX-antenna element is switched in the same 3.2 μs interval, no undistorted 1.6 μs window may be found, depending on the offset between the TX- and RX-switching. This is due to the fact that the measurement chain is settling twice, once after switching the RX-antenna and once after switching the TX-antenna.

3) Estimation of CTF: Using a back-to-back calibration the frequency responses of the measurement system have been recorded during the measurement campaign. Since the frequency response of the chain LU TX-LU RX has a very small ripple, the CTF of this link can be estimated from the observed data using a least-squares (LS) approach, see [11].

Since the frequency response of the TKK-RX has a large ripple within the used bandwidth, this LS approach cannot be used to estimate the MIMO-CTF for the link LU TX-TKK RX, due to significant noise-enhancement at the edges of the measured bandwidth. Therefore, a MMSE solution has been applied to estimate the MIMO-CTF for this link. The noise and signal covariance matrices have been estimated from the measured data. This is feasible since 63 measured channels, out of the 1024 channels, contain only realizations of the measurement noise.

3 Measurement Campaigns

Up to now we have performed four measurement campaigns with the above-described setup. The first three were carried out at the premises of LU (the third campaign is summarized in [10]). Here we report a sample result from the fourth measurement campaign performed in the computer science (CS) building of TKK, in September 2007, comprising an atrium and office rooms as shown in Fig. 4. The atrium is a large open hall akin to an airport terminal, or a part of a shopping mall. There are several bridges crossing the atrium on the second and third floor levels. The outer area of the atrium consists of modern offices. Parts of the measurements were done for office corridor scenario and for transitional channels from the atrium to office corridors. Four different RXs position were tested and for each combination the same routes were covered with the TX. *The total length of the measurement route accounted for* 4 *km, corresponding to more than* $160,000$ *MIMO snapshots for two links.*

The height of antennas was 1.8 m and 1.9 m for the LU and TKK RX, respectively, to imitate WLAN base station heights and 1.4 m for the LU TX. The movement of the TX was 0.6 m/s on average, hence 25 MIMO snapshots represents approximately 10 wavelengths.

4 Sample Results

Here we present narrow band signal-to-interference (SIR) results (no thermal noise) for one of the measured LOS scenarios ('route 5' in Fig. 4). We compare two different linear filtering methods at the RX (i) maximum-ratio-combining (MRC) [15] where the RX has knowledge of the channel matrix of the desired channel, $\mathbf{H}_1$, only and (ii) optimum linear filtering [16] where the RX has knowledge of both the channel matrix of the desired channel, $\mathbf{H}_1$, and of the interferer, $\mathbf{H}_2$. In order to study the spatial effects the channels are normalized as $\|\mathbf{H}_{1,k}\|_{\mathrm{F}}^2 = \|\mathbf{H}_{1,k}\|_{\mathrm{F}}^2 = M_R \cdot M_T$, where k is the frequency sub-channel and $\|\cdot\|_{\mathrm{F}}$ is Frobenius norm. The channel is not known at the TXs hence "omni" transmission is used, i.e., the weight to all the TX elements are identical for both the desired and the interfering TX, and the transmit weighting vector is not known to the RX, and at the TX the channel is not known, The SIR is

$$\gamma = \frac{S}{I} = \frac{\mathbf{w}^\dagger \mathbf{R}_1 \mathbf{w}}{\mathbf{w}^\dagger \mathbf{R}_2 \mathbf{w}}, \text{ where } \mathbf{R}_1 = \mathbf{H}_1^\dagger \mathbf{H}_1 \text{ and } \mathbf{R}_2 = \mathbf{H}_2^\dagger \mathbf{H}_2 \tag{1}$$

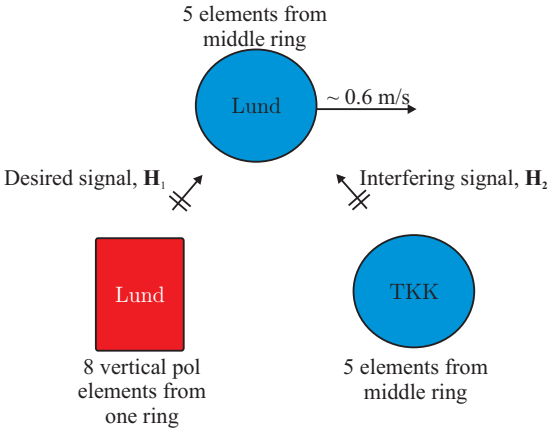

Fig. 5. Interference scenario.

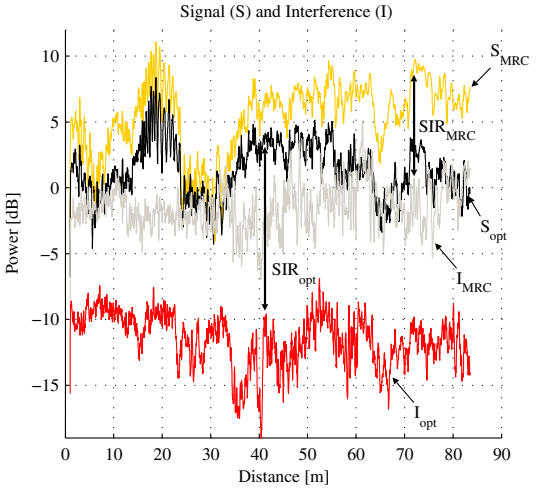

Fig. 6. Signal, interference and SIR results from Route 5 in Fig. 4.

Weight vector for MRC is well known and with $\mathbf{H}_1$ and $\mathbf{H}_2$ known at the receiver, the optimal linear weighting, $\mathbf{w} = \mathbf{V}_{\mathbf{A},1}$ where $\mathbf{V}_{\mathbf{A},1}$ is the eigenvector belonging to the largest eigen value of matrix $\mathbf{A} = \mathbf{R}_2^{-1}\mathbf{R}_1$. Fig. 6 shows the signal, interference, and SIR achieved over a sample measurement route (Route 5 in Fig. 4).

5 Conclusions

In this paper we presented measurement setup and sample results for dynamic multi-link wideband MIMO channel measurements. Two MIMO channel sounders from different institutions were used. Due to the somewhat different signaling structure, appropriate modifications of one of the receivers had to be performed. Using proper synchronization we obtained real-time measurement capability for a dual-link MIMO system that allows the investigation of joint dynamic effects (e.g., shadowing by a moving scatterer) on the two links. Sample results about the achievable signal-to-interference ratio demonstrated the capability of the setup. Future work will include evaluation of the measured data with respect to directional properties and link performance.

Acknowledgments

The research was funded by the WILATI project, a joint effort between three Scandinavian universities and is part of the NORDITE research programme, which is funded by Finnish, Swedish and Norwegian national research funding agencies Tekes, Vinnova and RCN, respectively.

References

[1] J. H. Winters, "On the capacity of radio communications systems with diversity in Rayleigh fading environments," *IEEE JSAC*, vol. 5, pp. 871–878, June 1987.
[2] I. E. Telatar, "Capacity of multi-antenna Gaussian channels," *Technical Memorandum, Bell Laboratories, Lucent Technologies*, October 1998, published in *European Transactions on Telecommunications*, vol. 10, no. 6, pp. 585–595, November/December 1999.
[3] G. J. Foschini and M. J. Gans, "On limits of wireless communications in fading environments when using multiple antennas," *Wireless Personal Communications*, vol. 6, no. 3, pp. 311–335, March 1998.
[4] G. Caire and S. Shamai, "On the achievable throughput of a multiantenna Gaussian broadcast channel," *IEEE Trans. on Information Theory*, vol. 49, no. 7, pp. 1691–1706, July 2003.
[5] W. Yu, W. Rhee, S. Boyd, and J. Cioffi, "Iterative water-filling for Gaussian vector multiple-access channels," *IEEE Trans. on Information Theory*, vol. 50, no. 1, pp. 145–152, January 2004.
[6] R. S. Blum, "MIMO capacity with interference," *IEEE JSAC*, vol. 21, no. 5, pp. 793–801, June 2003.
[7] S. Catreux, P. F. Driessen, and L. J. Greenstein, "Attainable throughput of an interference-limited multiple-input multiple-output (MIMO) cellular system," *IEEE Trans, on Communications*, vol. 49, no. 8, pp. 479–493, August 2001.
[8] G. J. Foschini, H. Huang, K. Karakayali, R. A. Valenzuela, and S. Venkatesan, "The value of coherent base station coordination," in *Proc. in Conference on Information Sciences and Systems (CISS 05)*, The Johns Hopkins University, March 2005, pp. 141–145.
[9] M. Jeng-Shiann Jiang; Demirkol, M.F.; Ingram, "Measured capacities at 5.8 GHz of indoor MIMO systems with MIMO interference," in *Proc. IEEE VTC-Fall*, vol. 1, October 2003, pp. 388–393.
[10] J. Koivunen, P. Almers, V.-M. Kolmonen, J. Salmi, A. Richter, F. Tufvesson, P. Suvikunnas, A. F. Molisch, and P. Vainikainen, "Dynamic multi-link indoor MIMO measurements at 5.3 GHz," in *Proc. European Conf. Antennas Propagat. (EuCAP '07)*, vol. CD-ROM, Edinburgh, UK, Nov. 2007, p. Tu2.9.7.
[11] R. Thoma, D. Hampicke, A. Richter, G. Sommerkorn, A. Schneider, U. Trautwein, and W. Wirnitzer, "Identification of time-variant directional mobile radio channels," *IEEE Trans. on Instrumentation and Measurement*, vol. 49, no. 2, pp. 357–364, April 2000.
[12] http://www.channelsounder.de/ruskchannelsounder.html.
[13] P. Almers, S. Wyne, F. Tufvesson, and A. F. Molisch, "Effect of random walk phase noise on MIMO measurements," in *Proc. IEEE VTC-Spring*, vol. 1, 2005, pp. 141–145.
[14] V.-M. Kolmonen, J. Kivinen, L. Vuokko, and P. Vainikainen, "5.3-GHz MIMO radio channel sounder," *IEEE Trans. on Instrumentation and Measurement*, vol. 55, no. 4, pp. 1263–1269, Aug. 2006.
[15] D. G. Brennan, "Linear diversity combining techniques," in *Proc. IRE*, vol. 47, June 1959, pp. 1075–1102.
[16] J. E. Hudson, *Adaptive Array Principles*, 3rd ed. Peter Peregrinus Ltd., London, UK, 1981.